Improving quantum interferometry by using entanglement

G. M. D'Ariano,[1,2] Matteo G. A. Paris,[1] and Paolo Perinotti[3]

[1]*Quantum Optics & Information Group, INFM Unità di Pavia, Pavia Italy*
[2]*Department of Electrical and Computer Engineering, Northwestern University, Evanston, Illinois 60208*
[3]*Dipartimento di Fisica and Sezione INFN, Universita di Milano, Milano Italy*

We address the use of entanglement to improve the precision of generalized quantum interferometry, i.e., of binary measurements aimed to determine whether or not a perturbation has been applied by a given device. For the most relevant operations in quantum optics, we evaluate the optimal detection strategy and the ultimate bounds to the minimum detectable perturbation. Our results indicate that entanglement-assisted strategies improve the discrimination in comparison with conventional schemes. Possible implementations of entanglement-assisted schemes, in order to approach the performances of the optimal strategies, are also suggested.

I. INTRODUCTION

An interferometric setup is devised to reveal minute perturbations to a given configuration. Such perturbations may be induced by the environment or by the action of a given device. In an interferometer, the internal quantum operation is monitored by probing the output state, which, in turn, results from the evolution of a given input. By suitably choosing the input signal and the detection stage one optimizes the interferometric measurement. Optimization has two main goals: (i) to maximize the probability of revealing a perturbation, when it occurs, and (ii) to minimize the value of the smallest perturbation that can be effectively detected.

In essence, an interferometric scheme may be viewed as a binary communication system [1,2], with the perturbation playing the role of the encoded information. In order to see better this analogy let us consider the scheme shown in Fig. 1(a). A source S of quantum states prepares the input signal, say ϱ_0, which travels along the interferometer, and it is eventually measured by some detector, denoted by D. The detector is described by the positive operator-valued measure (POVM) $\Pi(x)$, with $x \in X$, X being the manifold describing the possible detection outcomes. Inside the interferometer we have a generic quantum device, which may or may not perturb the signal, i.e., it performs the quantum operation described by the positive U_λ. If a perturbation occurs the signal is modified and, at the output, we have the state $\varrho_\lambda = U_\lambda \varrho_0 U_\lambda^\dagger$. The aim of the detection stage is to discriminate between ϱ_0 and its perturbed version ϱ_λ. An optimized interferometer is a device that is able to tell which ϱ, for λ as small as possible. Posed in this way, interferometry is naturally viewed as a binary decision problem, and the detection stage can be described by a two-value POVM $\{\Pi_0, \Pi_\lambda \equiv \mathbb{I} - \Pi_0\}$, whose realizations correspond to the two possible inferences.

The main goal of the present paper is to demonstrate the benefit of entanglement in binary interferometry. We will show that distinguishability of the two hypotheses ($\mathcal{H}_0$: nothing happened and $\mathcal{H}_\lambda$: a perturbation has occurred) can be improved by: (i) using an input signal that is entangled with another subsystem, and (ii) measuring the two systems jointly at the output of the interferometer [see Fig. 1(b)].

In order to optimize the detection strategies, and to show the benefit of entanglement, we will make use of results and methods from quantum detection theory applied to binary decision [3,4]. This approach is particularly useful for our purposes, since it does not refer to any specific detection scheme for the final stage of the interferometer, but rather, owing to its generality, it allows one to find the ultimate quantum limits to interferometry for specific classes of quantum signals.

In Sec. II, in order to establish notation, we briefly review the Neyman-Pearson approach to quantum binary decision, and state a lemma about minimum input-output overlap. Then, in Sec. III, we apply these results to the interferometric detection of perturbations induced by the most relevant operations in quantum optics such as displacement, squeezing, mixing, and phase shifting. As we will see, entanglement-assisted interferometers provide better discrimination than conventional schemes. In Sec. IV, we analyze possible implementations of entangled-assisted schemes, in order to approach, for the quantum operations discussed in Sec. III, the ultimate bounds to precision. Finally, in Sec. V we close the paper with some concluding remarks.
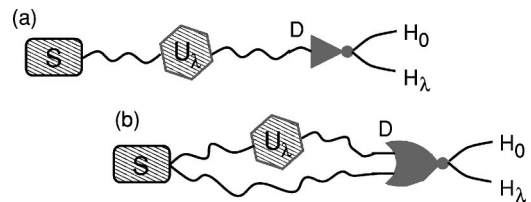

FIG. 1. A generalized interferometer is a binary detection scheme aimed at checking whether or not a given quantum device (the hexagon in the figure) has performed the quantum operations described by the unitary operator U_λ. The signal employed as a probe is prepared by the source S and then enters the device, which may or may not apply U_λ. The two hypotheses: $\mathcal{H}_0$ (the signal is unperturbed) and $\mathcal{H}_\lambda$ (U_λ has been applied) should be discriminated on the basis of the outcome of the detector D. (a) Simple scheme involving a single-mode probe. (b) Scheme involving an entangled probe.

II. QUANTUM BINARY DECISION IN THE NEYMAN-PEARSON APPROACH

The problem that we are facing is to decide between two hypotheses $\mathcal{H}_0$ and $\mathcal{H}_1$ about the state of a system, which is described by a density operator ϱ on the Hilbert space. To each hypothesis it will correspond a different density operator as follows:

$$\mathcal{H}_0: \quad \text{the system is in the state } \varrho_0,$$
$$\mathcal{H}_\lambda: \quad \text{the system is in the state } \varrho_\lambda. \quad (1)$$

Of course, there are many different measurements that can provide information about the state of the system: each of them, however, can be recast mathematically as a two-value POVM, corresponding to the two possible inferences $\mathcal{H}_0$ and $\mathcal{H}_1$, namely,

$$\Pi_0, \Pi_\lambda \geq 0, \quad \Pi_0 + \Pi_\lambda = \mathbb{I}. \quad (2)$$

One then needs an optimization strategy in order to determine the most reliable measurement discriminating between the two states. If ϱ_0 and ϱ_λ are orthogonal, i.e., $\varrho_0 \varrho_\lambda = \varrho_\lambda \varrho_0 = 0$ the solution is trivial, since Π_0 is the projection into any subspace that contains the support of ϱ_0 and is orthogonal to the support of ϱ_λ, and Π_λ is simply the complement $\Pi_\lambda = \mathbb{I} - \Pi_0$. In most cases of interest, however, the states are not orthogonal and one has to apply an optimi-

zation strategy. Since interferometric schemes are frequently used for detecting low-rate events, we may want to look for a strategy that keeps a low-rate of false alarm, namely, of wrong inference of perturbation occurrence. For this purpose, it is suitable to adopt a so-called Neyman-Pearson (NP) detection strategy, which consists in fixing a tolerable value of the false-alarm probability Q_0—the probability of inferring that the state of the system is ϱ_λ while it is actually ϱ_0—and then maximizing the detection probability Q_λ, i.e., the probability of a correct inference of hypothesis $\mathcal{H}_\lambda$ [5]. It has been proved by Helstrom [3] and Holevo [4] that this problem can be solved by diagonalizing the operator

$$\varrho_\lambda - \mu \varrho_0, \quad (3)$$

μ playing the role of a Lagrange multiplier accounting for the bound of fixed false-alarm probability. According to Ref. [3] the optimal POVM is the one in which Π_λ is the projection onto the eigenspaces of (3) relative to positive eigenvalues and $\Pi_0 = \mathbb{I} - \Pi_\lambda$. Unfortunately, the diagonalization of (3) is generally not easy. However, when $\varrho_0 = |\psi_0\rangle\langle\psi_0|$ and $\varrho_\lambda = |\psi_\lambda\rangle\langle\psi_\lambda|$ are pure states it can be easily solved analytically, by expanding $|\psi_0\rangle$ and $|\psi_\lambda\rangle$ on the eigenvectors of the difference operator (3). In this way one can evaluate both Q_0 and Q_λ versus μ, and after eliminating μ from their expressions one obtains

$$Q_\lambda = \begin{cases} [\sqrt{Q_0 |\kappa|^2} + \sqrt{(1-Q_0)(1-|\kappa|^2)}]^2 & \text{for } 0 \leq Q_0 \leq |\kappa|^2, \\ 1 & \text{for } |\kappa|^2 < Q_0 \leq 1, \end{cases} \quad (4)$$

where $|\kappa|^2 = |\langle\psi_0|\psi_\lambda\rangle|^2 = |\langle\psi_0|U_\lambda|\psi_0\rangle|^2$ is the overlap between the two states. The detection probability is a decreasing function of the overlap—the smaller the overlap, the easier the discrimination—since one can reach detection probability 1 while keeping a low false-alarm probability. On the contrary, when the overlap approaches 1, one is forced to decrease the detection probability in order to keep the false-alarm probability small.

The optimal choice of the probe that minimizes the overlap depends on the eigenvalues of the unitary operation U_λ. In order to illustrate this, let us expand U_λ in terms of its eigenvectors $U_\lambda = \sum_j e^{i\varphi_j} |\varphi_j\rangle\langle\varphi_j|$ (with integrals replacing sums in case of continuous spectrum) and let us denote by $O(U_\lambda) = \min_\psi |\langle\psi|U_\lambda|\psi\rangle|^2$ the minimum overlap between the two possible outputs, as obtained by varying the probe state. Then we have the following *overlap lemma* [6,7]: the minimum overlap $O(U_\lambda)$ is given by the distance from the origin in the complex plane of the polygon whose vertexes are the eigenvalues of U_λ. Therefore, the overlap is either zero (if the polygon includes the origin) or it is given by

$$O(U_\lambda) = \cos^2 \frac{\Delta\varphi}{2}, \quad (5)$$

where $\Delta\varphi$ is the angular spread of the eigenvalues. Zero overlap can be achieved with a probe state that is given by a superposition of at least three eigenvectors of U_λ, corresponding to eigenvalues that make a polygon that encloses the origin (or, if they exist, by a superposition of two of them corresponding to diametrically opposed eigenvalues). Instead, if the minimum overlap is not zero, it is achieved by the optimal probe state given by

$$|\psi\rangle = \frac{1}{\sqrt{2}}(|\varphi_i\rangle + |\varphi_j\rangle), \quad (6)$$

with $\Delta\varphi = \varphi_i - \varphi_j$.

III. ENTANGLEMENT IN BINARY INTERFEROMETRY

In this section we compare the performances of single-mode [Fig. 1(a)] and entanglement-assisted binary interferometric schemes [Fig. 1(b)] in the detection of small perturbations induced by relevant quantum optical operations such as displacement, squeezing, mixing, and phase shifting. The comparison is made in terms of the detection sensitivity, namely, upon parametrizing the "size" of the perturbation—

whence the corresponding output state—by a coupling parameter λ. In other words, the comparison is made in terms of the minimum detectable value λ_{min} of λ corresponding to output states that can be effectively discriminated while keeping the *acceptance ratio* γ^* of the NP strategy large, namely, $\gamma^* \doteq Q_\lambda / Q_0 \gg 1$. We will employ the quantity λ_{min} as a measure of the sensitivity of the interferometric scheme. Using Eq. (4) the above condition can be written in terms of the overlap as follows:

$$|\kappa|^2 = 1 - \Lambda(Q_0, \gamma^*),$$

$$\Lambda(Q_0, \gamma^*) = Q_0[1 + \gamma^*(1 - 2Q_0)$$
$$- 2\sqrt{\gamma^*(1 - Q_0)(1 - \gamma^* Q_0)}]. \qquad (7)$$

For each class of transformations, we will make some general considerations and then focus our attention on sensitivity bounds that can be achieved using probe signals that are feasible with current technology.

A. Perturbation made of a single-mode complex displacement

Let us first consider the case when the perturbation is imposed by the displacement operator $U_\alpha \equiv D(\alpha) = \exp(\alpha a^\dagger - \bar{\alpha} a)$. In principle, in this case, the discrimination can be done exactly with single-mode probe. This can be seen by writing the displacement as $U_\alpha = \exp(i2|\alpha| x_\theta)$, $x_\theta = 1/2(a^\dagger e^{i\theta} + a e^{-i\theta})$ being the quadrature operator, and $\theta = \arg(\alpha) + \pi/2$. Since the spectrum of the quadrature coincides with the real axis, the spectrum of U_α covers the whole unit circle, and, therefore, the states $|\psi_0\rangle$ and $|\psi_\alpha\rangle = U_\alpha |\psi_0\rangle$ can be discriminated with certainty either by choosing $|\psi_0\rangle$ as the eigenstate of the conjugated quadrature $x_{\theta + \pi/2}$, or, according to the overlap lemma, as a superposition of at least two eigenstates of the quadrature x_θ. Unfortunately, such optimal states are unphysical, since they are not normalizable and have infinite energy. Moreover, even though we approximate them with physical states with finite energy, the identification of the optimal states would require the knowledge of the phase of the perturbation. In order to see that, let us rewrite the eigenvector $|0\rangle_{\theta + \pi/2}$ as the limiting case of a squeezed vacuum, $|0\rangle_{\theta + \pi/2} = \lim_{|\zeta| \to \infty} |\zeta\rangle = \lim_{|\zeta| \to \infty} S(\zeta)|0\rangle$, where $\theta = \arg(\zeta) + \pi/2$ is the argument of the squeezing parameter ζ of the squeezing operator given by

$$S(\zeta) = \exp[1/2(\zeta a^{+2} - \bar{\zeta} a^2)], \qquad (8)$$

and $|0\rangle$ is the electromagnetic vacuum. Our squeezed vacuum has mean photon number $N = \sinh^2|\zeta|$. The overlap is readily evaluated as

$$|\kappa|^2 = |\langle \zeta | D(\alpha) | \zeta \rangle|^2$$
$$= \exp\{-|\alpha|^2[2N + 1 + \sqrt{N(N+1)} \cos 2\delta]\}, \qquad (9)$$

where $\delta = \arg(\zeta) - \arg(\alpha)$. By inserting the overlap in Eq. (7) we obtain the minimum detectable $|\alpha|^2$. However, Eq. (9) shows a very strong dependence of $|\alpha|^2_{min}$ on the phase pa-

rameter δ, which makes the whole optimized scheme very unstable, namely, one should know the phase of perturbation very precisely in order to get a truly optimized detection. Indeed, we have

$$|\alpha|^2_{min} \overset{N \gg 1}{\simeq} \Lambda(Q_0, \gamma^*)/4N \quad \text{for } \delta = \pi/2, \qquad (10)$$

$$|\alpha|^2_{min} \overset{N \gg 1}{\simeq} 4N\Lambda(Q_0, \gamma^*) \quad \text{for } \delta = 0, \qquad (11)$$

with the second expression that shows an asymptotically divergent behavior in N.

Let us now consider an entanglement-assisted scheme, where one has available a two-mode probe state $|\psi\rangle$ and take the configuration $U_\alpha = D(\alpha) \otimes \mathbb{I}$ in which the displacement perturbs one mode, say a, and the other mode is left unperturbed. At the probe state we consider the entangled state from parametric down-conversion of vacuum for finite gain—the so-called "twin-beam" state

$$|x\rangle\rangle = \sqrt{1 - x^2} \sum_n x^n |nn\rangle\rangle, \quad 0 \leq x < 1, \qquad (12)$$

where $|nn\rangle\rangle = |n\rangle_a \otimes |n\rangle_b$. The twin beam in Eq. (12) has mean photon number $N = 2x^2/(1 - x^2)$ and it is achieved starting from the vacuum via the unitary evolution $|x\rangle\rangle = \exp[x(a^\dagger b^\dagger - ab)]|0\rangle\rangle$. In order to evaluate the sensitivity, the main task is now to calculate the overlap $|\kappa|^2 = |\langle\langle x | U_\alpha | x \rangle\rangle|^2$. We have

$$\kappa = (1 - x^2) \sum_{m=0}^{\infty} \sum_{n=0}^{\infty} x^{m+n} \langle\langle mm | D(\alpha) \otimes \mathbb{I} | nn \rangle\rangle$$

$$= (1 - x^2) \sum_{n=0}^{\infty} x^{2n} \langle n | D(\alpha) | n \rangle$$

$$= (1 - x^2) e^{-(1/2)|\alpha|^2} \sum_{n=0}^{\infty} x^{2n} L_n(|\alpha|^2)$$

$$= \exp\left[-\frac{|\alpha|^2}{2} \frac{1 + x^2}{1 - x^2}\right] = \exp\left[-\frac{|\alpha|^2}{2}(N+1)\right], \qquad (13)$$

where $L_n(x)$ is the nth Laguerre polynomial. Equation (13) implies for $|\alpha|^2_{min}$ the scaling

$$|\alpha|^2_{min} \simeq \frac{\Lambda(Q_0, \gamma^*)}{N + 1}, \qquad (14)$$

which is independent on the phase of perturbation, and thus represents a robust bound to the sensitivity of a single-mode displacement.

B. Perturbation made of a single-mode squeezing (phase-sensitive amplifier)

The second kind of perturbation that we analyze is the squeezing of a single radiation mode, which is described by the squeezing operator $S(\zeta)$ in Eq. (8). Without loss of gen-

erality we can consider $\zeta = \bar{\zeta} = r$ as real and use the notation U_r to indicate the transformation, namely, $U_r = \exp[-irA]$, with $A = i/2(a^{+2} - a^2)$. The spectrum of A is continuous [8] and extends over the whole real axis. This means that the eigenvalues of U_r cover the whole unit circle. Therefore, it is possible, in principle, to discriminate the perturbation exactly, using as a probe either an eigenstate of the operator conjugated to A, or using a superposition of two or more eigenstates of A. However, analogously to the case of the displacement, such probe states are not normalizable and have infinite energy, whence one must resort to physical approximations of such states. For a coherent probe the overlap can be calculated through the overlap of the corresponding Wigner functions, giving as a result

$$|\langle \alpha | U_r | \alpha \rangle|^2 = \exp\left[-\frac{2N \cos^2\phi(1 - \cosh r - \sinh r)^2}{1 + \exp(2r)} - \frac{2N \sin^2\phi(1 - \cosh r + \sinh r)^2}{1 + \exp(-2r)} \right], \quad (15)$$

where $N = |\alpha|^2 = \langle \alpha | a^\dagger a | \alpha \rangle$ is the mean number of photons of the probe state. By expanding for small r we have

$$|\langle \alpha | U_r | \alpha \rangle|^2 \simeq 1 - Nr^2, \quad (16)$$

and, therefore, the minimum detectable perturbation would be

$$r_{min} \simeq \sqrt{\frac{\Lambda(Q_0, \gamma^*)}{N}}. \quad (17)$$

For a squeezed vacuum probe $S(\zeta)|0\rangle$ one has [9]

$$\kappa = \langle 0 | S^\dagger(\zeta) U_r S(\zeta) | 0 \rangle$$
$$= [\cosh r + 2i \sinh|\zeta|\cosh|\zeta|\sinh r \sin \psi]^{-1/2}, \quad (18)$$

where $\psi = \arg(\zeta)$ and correspondingly the minimum detectable r is given by

$$r_{min} = \begin{cases} \ln\left(\frac{1}{1 - \Lambda(Q_0, \gamma^*)} \{1 - \sqrt{\Lambda(Q_0, \gamma^*)[2 - \Lambda(Q_0, \gamma^*)]}\} \right) & \text{for } \sin \psi = 0, \\ \sqrt{\frac{\Lambda(Q_0, \gamma^*)}{2}} \frac{1}{N \sin \psi} & \text{otherwise,} \end{cases} \quad (19)$$

with $N = \sinh^2|\zeta|$. Again, the bound in Eq. (19) strongly depends on the phase between the squeezing perturbation and the squeezing of the probe, and, therefore, cannot be achieved in practice without prior knowledge of the phase of the perturbation.

Let us now consider an entangled probe state in a twin-beam state of the form given by Eq. (12). The input-output overlap is calculated as follows:

$$\kappa = \langle\langle x | U_r \otimes \mathbb{I} | x \rangle\rangle = (1 - x^2) \sum_{n=0}^{\infty} x^{2n} \langle n | U_r | n \rangle. \quad (20)$$

In order to calculate the matrix element $\langle n | U_r | n \rangle$ we use the identities

$$U_r = e^{(1/2)\tanh(r)a^\dagger} [\cosh(r)]^{-a^\dagger a - 1/2} e^{-(1/2)\tanh(r)a}$$

and

$$e^{-1/2 \tanh(r)a} |n\rangle = \sum_{l=0}^{[n/2]} \frac{[-\tanh(r)]^l}{2^l l!} \sqrt{\frac{n!}{(n-2l)!}} |n-2l\rangle, \quad (21)$$

where $[m]$ indicates the integer part of m, and finally we get

$$\langle n | U_r | n \rangle = \frac{n!}{[\cosh(r)]^{(n+1/2)}} \sum_{l=0}^{[n/2]} \frac{(-1)^l [\sinh(r)]^{2l}}{4^l (l!)^2 (n-2l)!}. \quad (22)$$

Using Eq. (22) we calculate κ by means of Eq. (20),

$$\kappa = (1 - x^2) \sum_{n=0}^{\infty} x^{2n} \frac{n!}{[\cosh(r)]^{(n+1/2)}} \sum_{l=0}^{[n/2]} \frac{(-1)^l [\sinh(r)]^{2l}}{4^l (l!)^2 (n-2l)!}$$

$$= \frac{(1 - x^2)}{[\cosh(r)]^{1/2}} \sum_{l=0}^{\infty} \left(-\frac{x^4 \sinh^2(r)}{4 \cosh^2(r)} \right)^l \frac{2l!}{l!^2}$$

$$\times \sum_{n=0}^{\infty} \frac{(n+2l)!}{n! 2l!} \left(\frac{x^2}{\cosh(r)} \right)^n$$

$$= \frac{(1 - x^2)}{[(x^4 + 1)\cosh(r) - 2x^2]^{1/2}}.$$

Inserting this expression in Eq. (7) we have for r_{min} the scaling law

$$r_{min} \simeq 2 \sqrt{\frac{\Lambda(Q_0, \gamma^*)}{1 - \Lambda(Q_0, \gamma^*)}} \frac{1}{\sqrt{N^2 + 2N + 2}}$$

$$\simeq \sqrt{\frac{\Lambda(Q_0, \gamma^*)}{1 - \Lambda(Q_0, \gamma^*)}} \frac{2}{N}. \quad (23)$$

The same result is obtained by varying the phase of the squeezing amplitude ζ, i.e., for complex r, thus confirming the robustness of the bound (23) that is obtained using an entangled probe.

C. Perturbation made of a two-mode phase shift

The third problem we address is that of a perturbation induced by the two-modes phase-shift operator $a^\dagger b + a b^\dagger$, characterizing a mixer (beam splitter) or a Mach-Zehnder interferometer. This case differs from the previous ones in that the perturbation is represented by the two-modes unitary operator $V_\phi = \exp\{i\phi(a^\dagger b + a b^\dagger)\}$. In this case the spectrum is given by $\exp\{im\phi\}$, with $m \in \mathbb{Z}$ (see, e.g., Ref. [10]). Therefore, if $\phi = (q/p)\pi$ with $q \in 2\mathbb{Z}+1$ and $p \in \mathbb{Z}$ (but this is a null-measure set of values of ϕ) then the optimal state is given by a superposition of two eigenstates of V_ϕ with eigenvalues differing by π. In the general case, the optimal state is any superposition of three or more eigenstates of V_ϕ, such that the polygon of its eigenvalues on the unit circle encloses the origin [7]. Such optimal states are entangled, since they are obtained from the eigenstates $|n,d\rangle\!\rangle$ of $a^\dagger a - b^\dagger b$,

$$(a^\dagger a - b^\dagger b)|n,d\rangle\!\rangle = d|n,d\rangle\!\rangle,$$

$$|n,d\rangle\!\rangle = \begin{cases} |n+d\rangle|n\rangle & \text{for } d \geq 0, \\ |n\rangle|n+|d|\rangle & \text{for } d < 0, \end{cases} \tag{24}$$

by the unitary transformation $\exp\{-(\pi/4)(a^\dagger b - a b^\dagger)\}$. Actually, the optimal states are far from being practically realizable. However, we have proved that they are entangled, and this suggests to explore the possibility of performing a reliable discrimination by physically realizable entangled states. For a twin beam we have

$$\kappa = \langle\!\langle x|V_\phi|x\rangle\!\rangle = (1$$

$$- x^2)\langle\!\langle 00|e^{xab}e^{i\gamma_0 a^\dagger b}e^{\{(1/2)\gamma_1(a^\dagger a - b^\dagger b)\}}e^{i\{\gamma_0 a b^\dagger\}}e^{x a^\dagger b^\dagger}|00\rangle\!\rangle, \tag{25}$$

where $\gamma_0 = \tan\phi$ and $\gamma_1 = -\ln(\cos^2\phi)$. After some algebra we get

$$|\kappa|^2 = \frac{1}{1 + \dfrac{4x^2 \sin^2\phi}{(1-x^2)^2}} = \frac{1}{1 + N(N+2)\sin^2\phi}. \tag{26}$$

The minimum detectable ϕ, according to Eq. (26), is thus given by

$$\phi_{min} = \arcsin\left(\frac{\Lambda(Q_0, \gamma^*)}{\sqrt{N(N+2)}}\right) \simeq \frac{\Lambda(Q_0, \gamma^*)}{N}. \tag{27}$$

The scaling in Eq. (27) does not depend on any parameter but the energy of the input state. This should be compared with the sensitivity of the customary single-mode interferometry [11] based on squeezed states, where the same scaling is achieved only for a very precise tuning of the phase of the
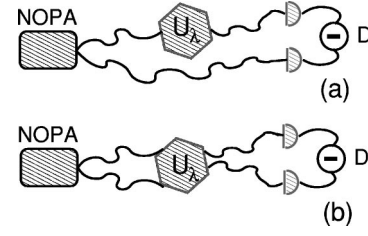

FIG. 2. Difference-photocurrent interferometric scheme to achieve ultimate bounds on precision by means of an entangled probe. The NOPA generates a twin beam that may be subjected to the action of the unitary U_λ. At the output the beams are detected and the difference photocurrent is measured. For an unperturbed interferometer the output is again a twin-beam state, and the scheme is designed in order to obtain a constant zero difference photocurrent, whereas a perturbation U_λ would produce fluctuations in the difference photocurrent. (a) Scheme for single-mode perturbation; (b) scheme for two-mode perturbation.

squeezing. This means that the entanglement-assisted interferometry provides a much more reliable and easily tunable scheme.

IV. IMPLEMENTATIONS OF ENTANGLEMENT-ASSISTED INTERFEROMETRIC SCHEMES

In this section we suggest two concrete schemes for binary decision based on an entangled probe. The schemes are feasible, at least in principle, and permit us to approach the ultimate precision bounds that have been obtained in the preceding section.

A. Entanglement in difference-photocurrent interferometry

In Fig. 2 we show a schematic diagram of a difference-photocurrent interferometer. The input state is the entangled twin-beam $|x\rangle\!\rangle$ produced by a nondegenerate optical parametric amplifier. Such entangled probe is possibly subjected to the action of the unitary U_λ [Figs. 2(a) and 2(b) describe the cases of a single mode and of a two-mode perturbation, respectively]. At the output the two beams are detected and the difference photocurrent $D = a^\dagger a - b^\dagger b$ is measured. If no perturbation occurs, then the output state is still a twin beam, and since $|x\rangle\!\rangle$ is an eigenstate of D with zero eigenvalue we have a constant zero outcome for the difference photocurrent. On the other hand, when a perturbation occurs the output state is no longer an eigenstate of D, and we detect fluctuations, which signal the presence of the perturbation itself. The false-alarm and the detection probabilities are given by

$$Q_0 = P(d \neq 0|\text{NOT}U_\lambda) \equiv 0, \tag{28}$$

$$Q_\lambda = P(d \neq 0|U_\lambda) = 1 - P(d \equiv 0|U_\lambda), \tag{29}$$

where the probability of observing zero counts at the output, after the action of U_λ, is given by

$$P(d \equiv 0|U_\lambda) = \sum_n |\langle\!\langle n,n|U_\lambda|x\rangle\!\rangle|^2, \tag{30}$$

since the eigenvalue $d=0$ is degenerate. In this scheme the false-alarm probability is zero and, therefore, it is not necessary to introduce an acceptance ratio. The scaling of the minimum detectable perturbation can be obtained directly in terms of the detection probability Q_λ by Eqs. (29) and (30). For the single-mode transformations considered in the preceding section we have

$$P(d=0|\alpha\neq0)=\exp[-|\alpha|^2(1+N)]I_0[|\alpha|^2\sqrt{N(N+2)}]$$
(31)

for the displacement, where $I_0(x)$ is the zeroth modified Bessel function, and

$$P(d=0|r\neq0)=1-r^2N+O(r^2)\frac{\sqrt{Q_\lambda}}{N}$$
(32)

for the squeezing. The minimum detectable perturbations are thus given by

$$|\alpha|^2_{min}\simeq\frac{\sqrt{Q_\lambda}}{N},\quad r_{min}\simeq\frac{\sqrt{Q_\lambda}}{N}.$$
(33)

For the two-mode phase-shift transformation we have

$$P(d=0|\phi\neq0)=1-\frac{1}{2}\phi^2N^2+O(\phi^2)\;\rightarrow\;\phi_{min}\simeq\frac{\sqrt{2Q_\lambda}}{N}.$$
(34)

One can see that in all examples considered above, an interferometer based on a difference-photocurrent measurement provides a precision that rescales with the energy in the same way as the ultimate bounds obtained in the preceding section.

It is worth noticing that the experimental measurement of a modulated absorption based on entanglement-assisted difference-photocurrent detection has been already performed using the entangled beam exiting an amplifier above threshold (optical parametric oscillator, OPO) [12].

B. Effects of nonunit quantum efficiency

Since the setup analyzed in the preceding section is aimed for a possible implementation, it is worth analyzing the effect of nonunit quantum efficiency in the detection stage. We will consider the case of the estimation of a displacing amplitude. The other perturbations may be treated in an analogous way.

In case of nonunit quantum efficiency the statistics of each detector of Fig. 2 is described by the POVM

$$\Pi_\eta(m)=\sum_{n=m}^{\infty}\Pi(n)\binom{n}{m}\eta^m(1-\eta)^{n-m},$$
(35)

which is a Bernoullian convolution of the ideal POVM of a photocounter $\Pi(n)=|n\rangle\langle n|$. This means that the probability distribution of the outcomes for the difference photocurrent D is given by

$$P_\eta(d)=\begin{cases}\sum_n\text{Tr}[\varrho\Pi_\eta(n+d)\otimes\Pi_\eta(n)],&d\geqslant0,\\[12pt]\sum_n\text{Tr}[\varrho\Pi_\eta(n)\otimes\Pi_\eta(n+d)],&d<0,\end{cases}$$
(36)

where ϱ is the outgoing state (either ϱ_0 or ϱ_λ). The main effect of quantum efficiency is the occurrence of nonzero output also in the case of no perturbation, i.e., the appearance of a false-alarm probability

$$Q_0\equiv P(d\neq0|\alpha=0)=1-\sum_{d>0}\sum_n\langle\!\langle x|\Pi_\eta(n+d)\otimes\Pi_\eta(n)$$
$$+\Pi_\eta(n)\otimes\Pi_\eta(n+d)|x\rangle\!\rangle,$$
(37)

whereas the detection probability is given by

$$Q_\alpha\equiv1-P(d=0|\alpha\neq0)$$
$$=\sum_n\langle\!\langle x|D^\dagger(\alpha)\Pi_\eta(n)\otimes\Pi_\eta(n)D(\alpha)|x\rangle\!\rangle.$$
(38)

Equation (37) would suggest a slight modification of the detection strategy, where the inference of $\mathcal{H}_0$ is associated with a difference photocurrent whose absolute value is under a threshold value d^*. We have numerically calculated Q_0 and Q_α for different (integer) values of the threshold and obtained the plots in Fig. 3. The plots represent the characteristics $Q_\alpha(Q_0)$ for different values of the entanglement parameter x for quantum efficiency equal to $\eta=0.9$ and $\eta=0.75$, respectively. The perturbation intensity is given by $|\alpha|=0.7$. Apart from the trivial point $Q_0=Q_\alpha=1$, corresponding to a threshold $d^*=0$, for any value of the parameter x we have a sequence of points, corresponding to the integer values of the threshold $d^*, d^*\in\mathbb{N}$. The highest value of Q_α corresponds to maximum entanglement, and to the threshold $d^*=1$, i.e., to our original strategy that associates a perturbation to every outcome d different from zero. By employing an acceptance ratio criterion, the optimal strategy is the one that has the highest detection probability Q_α, provided that the ratio Q_α/Q_0 is higher than a fixed value γ^*. This criterion can be viewed in the Q_0, Q_α plane as looking for the highest point lying over the line $Q_\alpha=\gamma^*Q_0$.

In Fig. 3 the horizontal line corresponds to the value of Q_α obtained for unentangled probe ($x=0$). In this case $Q_0=0$ and Q_α can be analytically calculated through Eq. (29). A systematic analysis shows that in the quantum regime of a small number of photons, the benefit of entanglement can be appreciated also in presence of nonunit quantum efficiency, i.e., the minimum detectable perturbation scales almost as in the ideal case. On the other hand, in the semiclassical regime of strong signal the scaling is degraded, as it happens for single-mode squeezed-assisted interferometry [13]. In this case, the main advantage of an entangled scheme concerns the stability with respect to phase fluctuations of the perturbation.
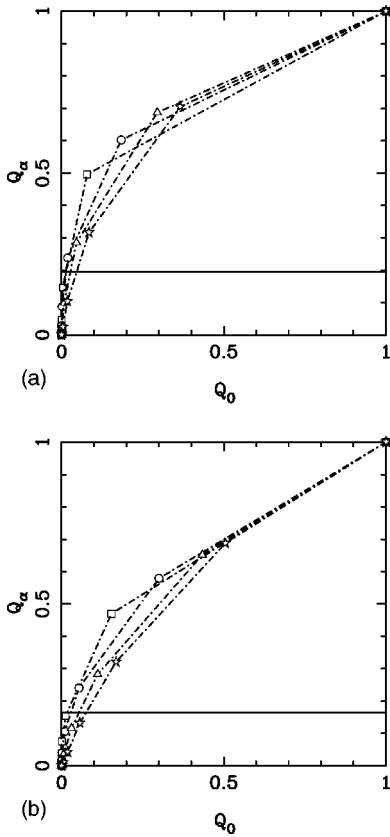
FIG. 3. Characteristic curves $Q_\alpha(Q_0)$ for the threshold strategy in difference-photocurrent interferometry. (a) Quantum efficiency $\eta=0.9$ and (b) $\eta=0.75$. In both plots, the horizontal curve corresponds to Q_α for a not entangled input. The data are for average number of photons in the twin-beam given by $N=1$ (squares), $N=2.8$ (circles), $N=5.2$ (triangles), and $N=8.0$ (stars).

C. Benefit of entanglement in heterodyne interferometry

In this section, we analyze heterodynelike interferometric schemes, i.e., schemes where the detection stage consists of the measurement of the real and the imaginary part of the complex photocurrent $Z=a+b^\dagger$, a and b being modes of the field. Such a measurement can be obtained by heterodyne, eight-port homodyne and six-port homodyne detectors. Besides being a possible implementation of entanglement-based measurement, the analysis of this setup allows for a direct comparison with the analog unentangled scheme. In Fig. 4 we show a schematic diagram of the detection setup (again, we consider the case of a displacement perturbation). Figure
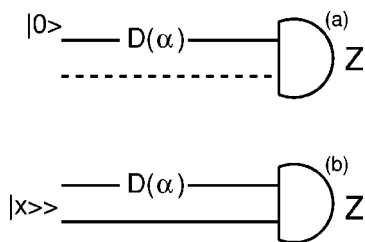

FIG. 4. Schematic diagram of a heterodynelike interferometer to detect an amplitude perturbation $D(\alpha)$.
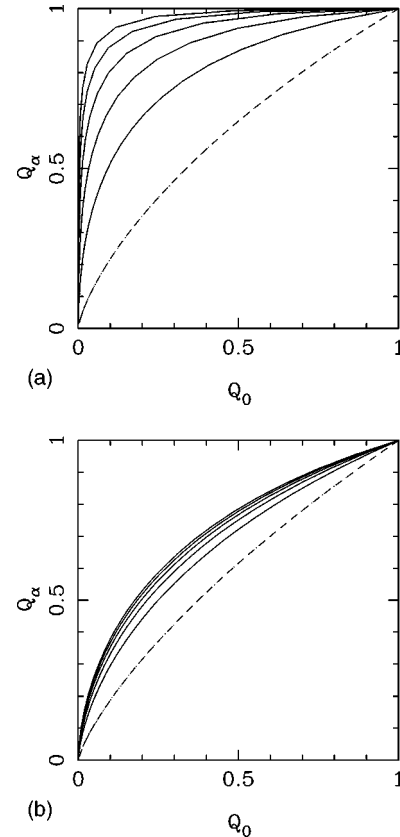

FIG. 5. Characteristic curves $Q_\alpha(Q_0)$ for the threshold strategy (40) in heterodyne interferometry. (a) Unit quantum efficiency and (b) $\eta=0.75$. In both plots the lower dashed curve corresponds to a not entangled input, whereas for increasing entanglement (from bottom to top $N=0,1,2,3,4,5$) we have improved characteristics. The perturbing amplitude is $|\alpha|=0.5$.

4(a) describes the customary single-mode scheme to estimate an unknown amplitude with the vacuum as unperturbed signal: actually this corresponds to the optimal single-mode measurement according to quantum estimation theory [3]. Figure 4(b) represents the scheme employing twin beam as input. Each heterodyne outcome consists of a pair of real numbers for the photocurrents $X=(Z+Z^\dagger)/2$ and $Y=(Z-Z^\dagger)/2i$. The probability distribution for the complex outcome $z=x+iy$ is given by $p_1(z|\alpha)=1/\pi|\langle z|\alpha\rangle|^2$ in the single-mode case and by $p_2(z|\alpha)=1/\pi|\langle\langle x|D^\dagger(\alpha)|z\rangle\rangle|^2$ for the entanglement-based scheme, where $|z\rangle\rangle=D(z)\Sigma_p|p\rangle|p\rangle$. Both probabilities are Gaussian and can be summarized as

$$p(z|\alpha)=\frac{1}{\pi\Delta_x^2}\exp\left\{-\frac{|z-\alpha|^2}{\Delta_x^2}\right\}, \quad \Delta_x^2=\frac{1-x}{1+x}+\frac{1-\eta}{\eta},$$

$$(39)$$

where η is the quantum efficiency of the photodetectors involved in the heterodyne (or multiport homodyne) detector [by putting $x=0$ in Eq. (39) we easily recover the single-mode case]. A binary inference from heterodyne data can be obtained by a threshold strategy as follows:
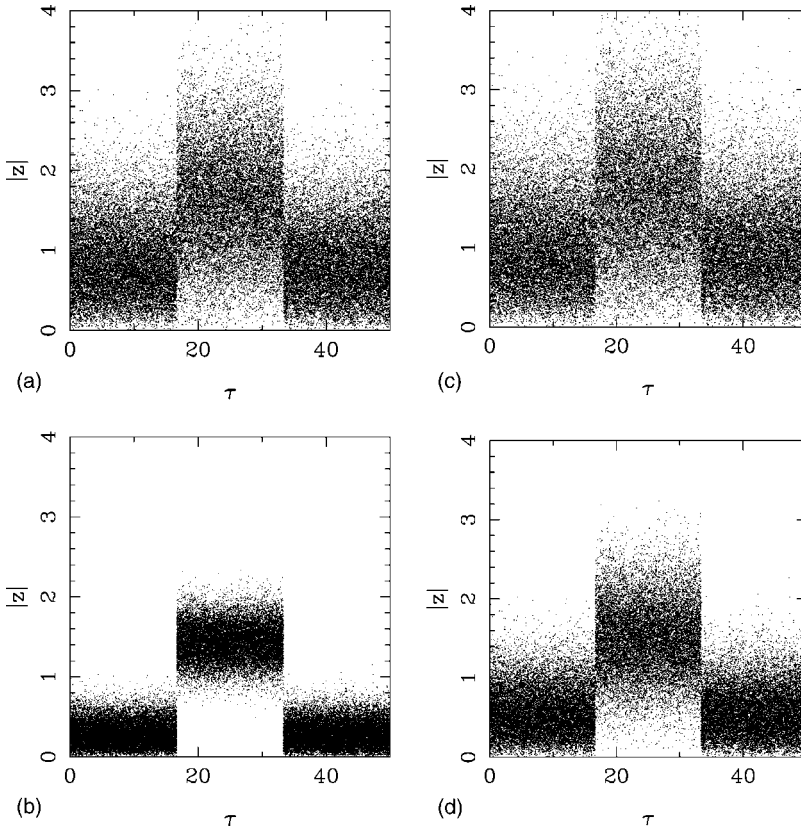
FIG. 6. Monte Carlo simulation of entangled-assisted heterodyne interferometry to detect an amplitude perturbation. The simulated data are reported as a function of an arbitrary rescaled time τ ($\tau=1$ corresponds to 1000 events) for an initially unperturbed system that is subjected to an amplitude perturbation $|\alpha|=1$ during a time interval $\Delta\tau=15$. We report the resulting outcome for not entangled [(a) and (c)] and entangled input [(b) and (d) $N=3.3$] both for unit quantum efficiency [(a) and (b)] and for $\eta=0.75$ [(c) and (d)].

$$\text{if } |z| < \Lambda \to \text{"no perturbation"}$$
$$\text{if } |z| \geq \Lambda \to \text{"perturbation"} \quad (40)$$

such that the false-alarm and the detection probability are given by

$$Q_0 = \int_{|z|\geq\Lambda} d^2z\, p(z|0), \quad Q_\alpha = \int_{|z|\geq\Lambda} d^2z\, p(z|\alpha). \quad (41)$$

By varying the threshold Λ we parametrically obtain the characteristics $Q_\alpha(Q_0)$ of the strategy (40). In Fig. 5 we report Q_α versus Q_0 for a small perturbing amplitude both in the ideal case and for quantum efficiency $\eta=0.75$. The different curves correspond to different degrees of entanglement at the input. As a matter of fact the characteristics are improved using entanglement, and the benefit of entanglement is still present in case of an imperfect detection stage. Remarkably, in the latter case the characteristics saturate for increasing values of x, which means that only a moderate entanglement is needed to achieve an optimal inference strategy.

We also performed a Monte Carlo simulation of the whole detection scheme. In Fig. 6 we report the simulated data as a function of an arbitrary rescaled time τ ($\tau=1$ means 1000 events) for an initially unperturbed system that is subjected to a tiny amplitude perturbation on a time interval $\Delta\tau=15$. We report the resulting outcome for entangled input and not entangled input both for unit quantum efficiency and for $\eta=0.75$. As it is apparent from the plots, using an entangled input results in a more distinguishable perturbation.

V. SUMMARY AND CONCLUSIONS

In this paper we have analyzed the effect of entanglement on the interferometric estimation of relevant quantum optical parameters such as displacing and squeezing amplitudes or interferometric phase shift. We have evaluated the minimum detectable perturbation according to the Neyman-Pearson detection strategy, and have shown that entanglement improves the detection in comparison with single-mode schemes. In particular, for the case of estimation of the displacement and the squeezing amplitudes we have shown that the precision of the apparatus that uses an entangled probe is independent of the phase of the perturbation, and is, therefore, more stable and reliable than a simple scheme based on single-mode probes. Similarly, the estimation of a two-mode phase shift is more stable when we use a twin beam than when using squeezed states.

Since the Neyman-Pearson detection strategy does not correspond to a realistic detector, we also analyzed possible implementations based on difference photocurrent and heterodyne interferometry using entangled twin beam. Remarkably, these schemes improve precision also in presence of nonunit quantum efficiency of the involved photodetectors. We conclude that the technology of entanglement can be of great help in improving precision and stability of quantum interferometers.

[1] J.N. Hollenhorst, Phys. Rev. D **19**, 1669 (1979).

[2] M.G.A. Paris, Phys. Lett. A **225**, 23 (1997).

[3] C.W. Helstrom, *Quantum Detection and Estimation Theory* (Academic Press, New York, 1976).

[4] A. S. Holevo, *Probabilistic and Statistical Aspects of Quantum Theory* (North-Holland, Amsterdam, 1982).

[5] J. Neyman and E. Pearson, Philos. Trans. R. Soc. London, Ser. A **321**, 289 (1933).

[6] K.R. Parthasarathy, in *Stochastics in Finite and Infinite Dimensions*, edited by Rajput *et al.*, Trends in Mathematics (Birkhauser, Boston, 2000), pp. 361–377.

[7] G.M. D'Ariano, P. Lo Presti, and M.G.A. Paris, Phys. Rev. Lett. **87**, 270404 (2001).

[8] C.G. Bollini and L.E. Oxman, Phys. Rev. A **47**, 2339 (2001).

[9] G.M. D'Ariano, Int. J. Mod. Phys. B **6**, 1291 (1992).

[10] G.M. D'Ariano, M.G.A. Paris, and P. Perinotti, J. Opt. B: Quantum Semiclassical Opt. **3**, 337 (2001).

[11] C.M. Caves, Phys. Rev. D **23**, 1693 (1981); R.S. Bondurant and J.H. Shapiro, *ibid.* **30**, 2548 (1984).

[12] P. Souto-Ribeiro *et al.*, Opt. Lett. **22**, 1893 (1997); J.R. Gao *et al.*, *ibid.* **23**, 870 (1998).

[13] M.G.A. Paris, Phys. Lett. A **201**, 132 (1995).